Encapsulation and Release of Molecular Cargos via Temperature-Induced Vesicle-To-Micelle Transitions

Qi Chen, Holger Schönherr, and G. Julius Vancso**

Temperature-induced vesicle-to-micelle transitions of polystyrene-block-poly acrylic acid (PS_{139}-b-PAA_{17}) aggregates in tetrahydrofuran (THF)/H_2O solvent mixtures are studied. For a typical system with an initial concentration of PS_{139}-b-PAA_{17} of 2 wt% and 50 vol% of H_2O, the morphology of the aggregates changes from vesicles to micelles upon heating from room temperature to 45 °C. The transition temperature is found to depend on the polymer concentration as well as solvent composition. A higher polymer concentration results in a higher transition temperature. The morphological change is attributed to a change in the solvent-polymer interactions, which results in a reduction in interfacial energy. The corresponding temperature-induced morphological change is employed as a strategy for the reversible release and encapsulation of small molecules. The release of Rhodamine 110 bisamide above the transition temperature is observed as a result of the trypsin-catalyzed hydrolysis of the bisamide into Rhodamine 110. Likewise, the successful encapsulation of Rhodamine 110 below the transition temperature is proven using sodium nitrite as a chemical quencher.

1. Introduction

Self-assembly of amphiphilic block copolymers (BCPs) in solution has received considerable attention in the past two decades.[1–4] Examples include, among others, BCP micelles and vesicles. The internal volume of BCP vesicles, also called "polymersomes", with their diameters between several hundreds to tens of nanometers is on the order of atto- to zepto-liters and enables the encapsulation of small numbers of hydrophilic molecules in the polymersome interior. BCP vesicles possess superior stability, toughness, and stiffness compared to their low-molecular-weight analogues, the liposomes,[5] because of the high molar mass of the BCPs. Therapeutically active compounds have been successfully encapsulated during the assembly of these superstructures, which is interesting in view of applications in the areas of drug delivery and cosmetics.[5] For real applications, triggered release of vesicle-encapsulated active substances is a prerequisite since the continuous loss of encapsulated compounds via diffusion is very slow due to the high molar mass of the BCPs.[6] Among the different stimuli for programmed drug delivery using polymersomes, temperature plays an important role, as reviewed very recently by Feijen and co-workers.[7]

Temperature itself is one determining factor in BCP self-assembly in solution.[8–11] For triggered release, polymersomes of BCPs containing a thermosensitive block, e.g., poly(*N*-isopropylacrylamide) (PNIPAM), have been widely studied. PNIPAM undergoes a phase transition from hydrophilic to hydrophobic at a lower critical transition temperature (LCST) of ~32 °C. At a temperature *lower* than the LCST, the temperature responsive vesicles dissociate to release the encapsulated substances.[12–14] A second example are vesicles made from polybutadiene-*block*-poly(L-lysine) (PBD-PLys)

Dr. Q. Chen, Prof. H. Schönherr, Prof. G. J. Vancso
Department of Materials Science and Technology of Polymers
University of Twente
MESA+ Institute for Nanotechnology
Postbus 217, 7500 AE Enschede, The Netherlands
E-mail: schoenherr@chemie.uni-siegen.de
g.j.vancso@tnw.utwente.nl

Prof. H. Schönherr
University of Siegen
Department of Physical Chemistry I
Adolf-Reichwein-Str. 2, 57076 Siegen, Germany

DOI: 10.1002/smll.201001348

small NANO MICRO

in basic solutions. The size of these vesicle *increased* upon increasing the temperature as a result from a transition of the PLys conformation from an α-helix to a β-sheet structure.[15] Another approach utilized hyperbranched poly[3-ethyl-3-(hydroxymethyl)oxetane]-*star*-poly(ethylene glycol) (HBPO-PEG) vesicles. The aqueous vesicle solution displayed unusual and reversible LCST transitions with an adjustable LCST from 8 to 81 °C. The transition of the vesicles is caused by the dehydration of the PEG block with increasing temperature.[16] A similar temperature-induced reversible phase change of polystyrene-*block*-poly(ethylene oxide) aggregates in a water and dimethyl formamide (DMF) mixed solvent system was observed using transmission electron microscopy (TEM) and dynamic light scattering (DLS).[17]

In our current report we expand these findings in an approach that exploits the temperature-induced *reversible* morphological changes of BCPs for *both* the encapsulation *and* release of functional molecules. Polymersomes of PS_{139}-*b*-PAA_{17} (PS-*b*-PAA) with diameters between 100 and 250 nm were prepared, and the temperature-induced vesicle-to-micelle transition was utilized to release and/or (re-)encapsulate Rhodamine 110 bis-(benzyloxy carbonyl-L-arginine amide) (R110-Arg_2). Our study complements the studies mentioned above,[12–16] which exploited the triggered release of encapsulated substances upon cooling of the vesicles. In the case of PS-*b*-PAA, substances are released from the vesicle interior upon heating and subsequently may react with compounds present in the solution outside the vesicles. In addition, upon cooling to room temperature, the reaction product is partially encapsulated in the reformed vesicles and is hence protected from unwanted reactions (**Scheme 1**).

2. Results and Discussion

2.1. Temperature-Induced Morphological Changes of PS-*b*-PAA Aggregates

To study the dependence of the PS-*b*-PAA aggregate morphologies on temperature, samples that were prepared by adding water into BCP solution in tetrahydrofuran (THF) were heated. An aliquot of the solution was taken out at a desired temperature and added into an excess amount of water to "freeze" the morphology. Typical TEM images of the samples taken at different temperatures are shown in **Figure 1**. The morphology of the aggregates with a BCP concentration of 2 wt% and water content of 50 vol% was vesicular at room temperature (Figure 1a). In contrast, at 60 °C the morphology could be described as micellar (Figure 1b). When the sample was subsequently cooled down to room temperature, the vesicular morphology was regenerated, indicating the reversibility of the process (Figure 1c).

The corresponding changes in size distribution were analyzed by DLS (Figure 1d). A bimodal distribution of

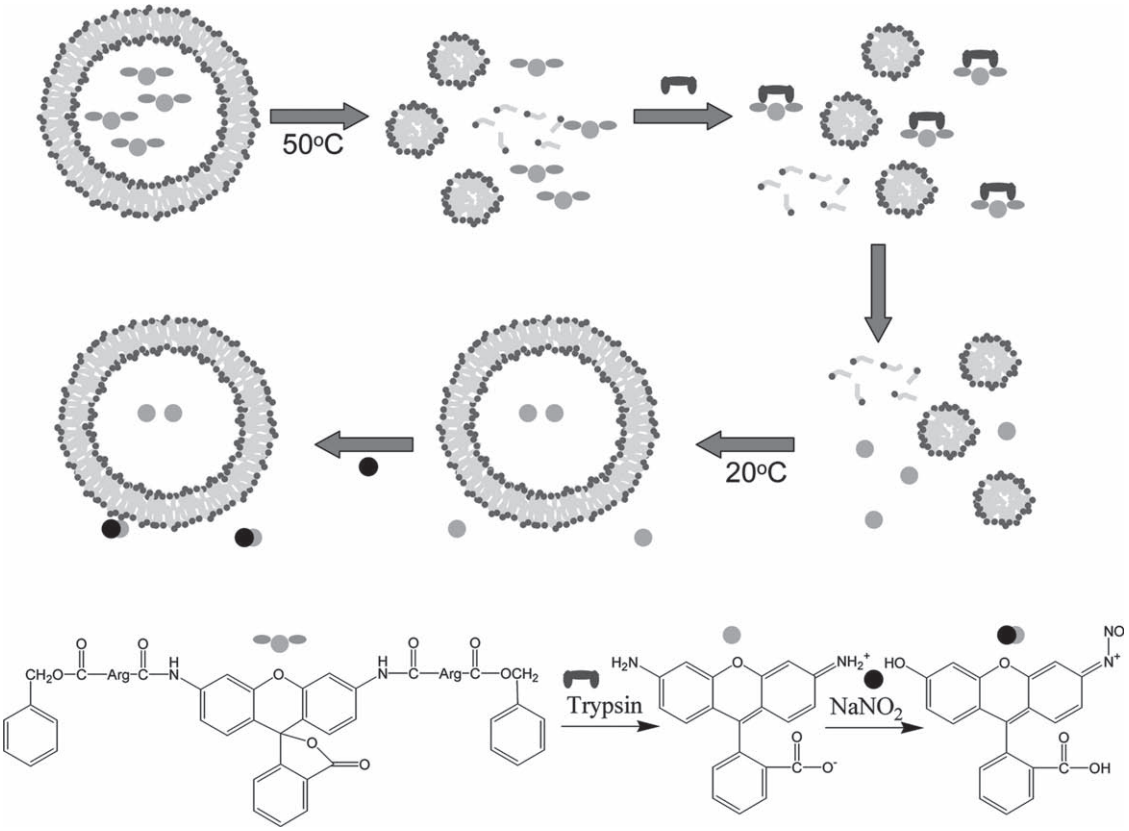

Scheme 1. Top: Schematic of the temperature-induced release and subsequent enzymatic attack on released R110-Arg_2 as well as the re-encapsulation of the reaction product R110, which is protected from added $NaNO_2$. Bottom: Formulas of the enzymatic and the quenching reactions.

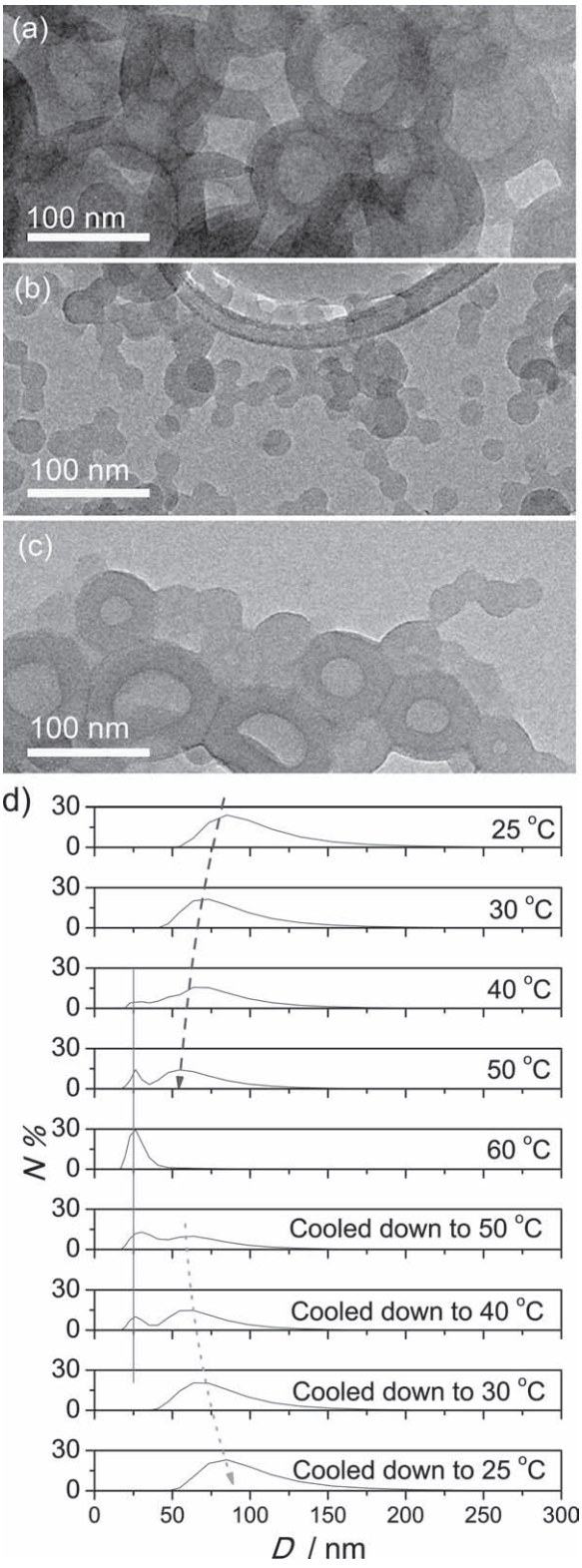

Figure 1. TEM images of PS-*b*-PAA aggregates (2 wt% in THF, water content 50 vol%) a) prepared at room temperature (25 °C), b) subsequently heated to 60 °C, and c) after cooling the solution in (b) back to 25 °C. d) Distribution of the diameter of the aggregates at different temperatures determined from DLS. The vertical solid line indicates the diameter of the micelles (25 nm), while the dashed and dotted curves serve as a guide to the eye indicating the most probable vesicle diameter at the corresponding temperature.

diameter (D) was observed for the sample heated at 50 °C. The peak at ~25 nm is attributed to the diameter of micelles as it corresponds to the wall thickness of the vesicles determined from TEM images (t = 25 ± 2 nm). At 60 °C the vesicle peak disappeared and the distribution showed a single maximum. The transition from a mono-modal to a bimodal distribution fully supports the above interpretation that a vesicle-to-micelle transition takes place when the temperature of the aggregates is raised to above ~40 °C in this case.

The morphological changes of other BCP systems were studied and reported previously in the literature.[16–18] In general, the interaction between the BCP and the solvent, represented by the interaction parameter χ, is affected by the temperature. It was reported that the change of BCP–solvent interaction, i.e., the change in solubility of the BCP, causes the vesicle-to-micelle transition at elevated temperature.[17]

To precisely determine the transition temperature, the turbidity of PS-*b*-PAA solutions was monitored using UV–vis spectroscopy. The absorbance at 400 nm of a system with 2 wt% PS-*b*-PAA concentration and 50 vol% of water was monitored when the sample was heated with a constant heating rate of 0.5 °C min^{-1}, as shown in **Figure 2**. The absorbance decreased slightly in the initial part of the trace, followed by a sudden decrease at temperatures above 40 °C. This decrease in turbidity is attributed to the vesicle-to-micelle transition. The transition temperature (here 45.3 ± 0.8 °C) was estimated from the inflection point of the plot by locating the minimum of the first derivative of the trace.

The transition temperature found may depend on various factors, including the heating rate, the polymer concentration and the solvent composition. These different determinants were investigated, as discussed below.

The effect of the heating rate on the transition temperature of the aggregates was studied for PS_{139}-*b*-PAA_{17} vesicles

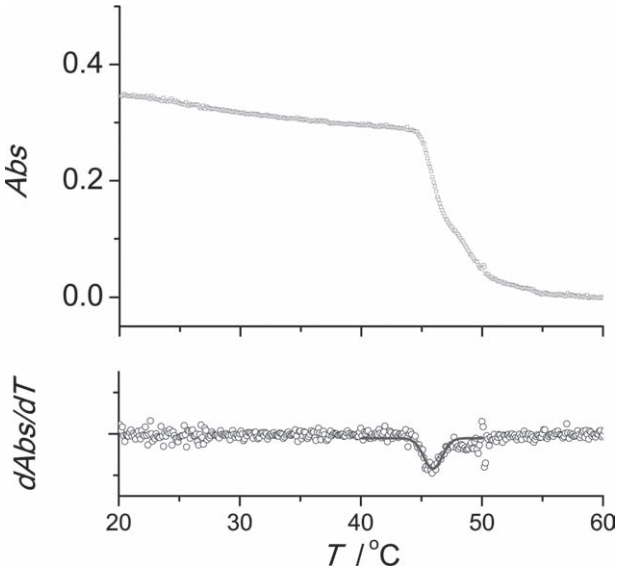

Figure 2. Turbidity of a solution of PS-*b*-PAA vesicles (2 wt% BCP in THF, H_2O 50 vol%) recorded as a function of temperature. The sudden decrease of turbidity represents the vesicle-to-micelle transition of the aggregates. The transition temperature is determined from the inflection point of the curve.

small NANO MICRO

with 1 wt% initial polymer concentration and 50 vol% H_2O. Samples with the same composition were heated from room temperature to 60 °C using different heating rates and the corresponding turbidity traces are shown in **Figure 3**a. The transition temperatures (T_c) determined from these data are plotted as a function of heating rate in Figure 3b.

The transition temperature was found to depend on the heating rate of the experiments. T_c increased from 34.7 to 53.3 °C as the heating rate changed from 0.1 to 30 °C min^{-1}. The value of T_c remained almost constant when the heating rate was below 5 °C min^{-1} as can be seen in the inset of Figure 3b and increased in a linear fashion when the heating rate was above 5 °C min^{-1}. In a study on the transition temperature of dioctadecyldimethyl ammonium bromide vesicles using differential scanning calorimetry (DSC) an increase of T_c was observed as a function of heating rate for heating rate ranging from 20 to 80 °C min^{-1}.[19] Unless otherwise mentioned, all further turbidity measurements were carried out with a heating rate of 0. 5 °C min^{-1}.

2.2. The Influence of Solution Composition on the Transition Temperature

The morphological changes of the PS-*b*-PAA aggregates with temperature for different initial polymer concentrations and THF content were followed by monitoring the turbidity as a function of temperature. The results are shown in **Figure 4**.

The critical transition temperature (T_c) of the system was found to increase as the initial polymer concentration of the system increased, as indicated by the dotted line in Figure 4a. Here the THF content of all systems was kept constant at 50 vol%. On the other hand, turbidity diagrams of systems

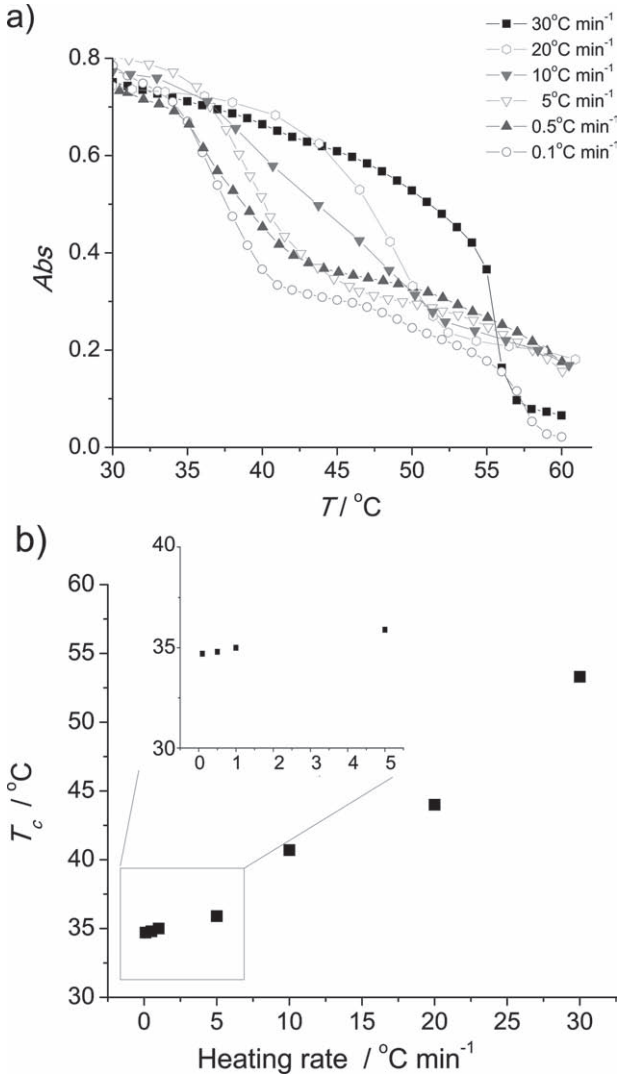

Figure 3. a) Turbidity of PS-*b*-PAA solutions (1 wt% BCP in THF, H_2O 50 vol%, D = 75 nm) as a function of temperature for different heating rates as indicated in the legend. b) Transition temperature plotted as a function of scanning rate. The inset is the zoom-in of the selected region.

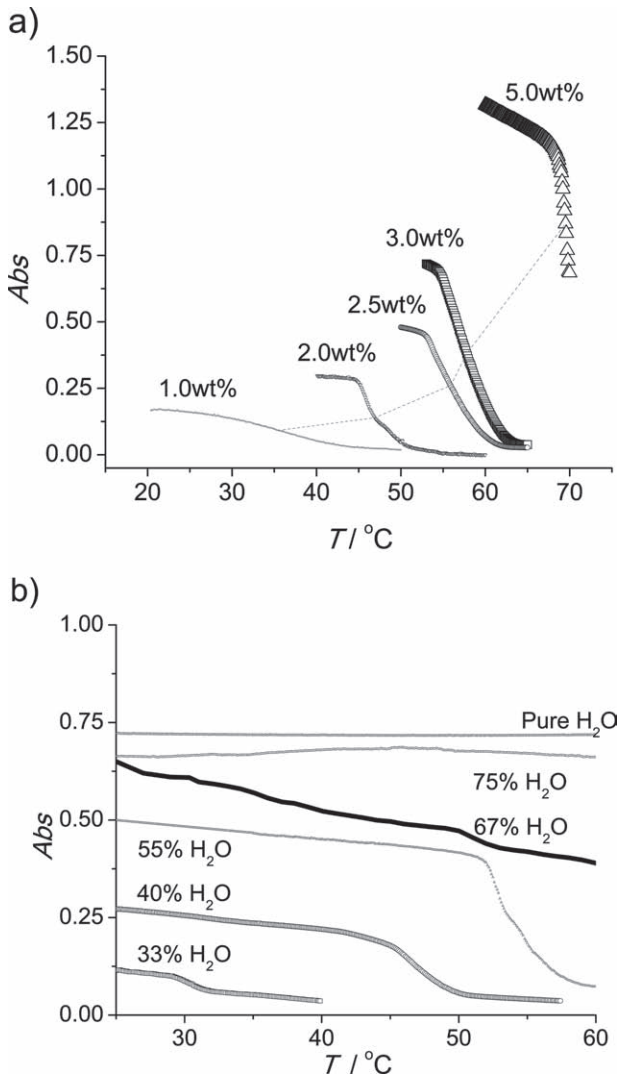

Figure 4. a) Turbidity versus temperature for PS_{139}-*b*-PAA_{17} solutions with different initial polymer concentrations as indicated in the graph and a constant solvent composition (50 vol% THF). b) Change in turbidity with temperature for PS_{139}-*b*-PAA_{17} vesicles with different THF/water percentages and a constant initial polymer concentration of 2 wt%.

with a constant 2 wt% initial polymer concentration and different THF contents (Figure 4b) showed that morphological changes did not occur until the THF fraction was above 40 vol%. The transition temperature was found to depend markedly on the THF content, a lower T_c was observed with increasing THF content. A similar effect was observed in the PS-*b*-PEO system with DMF as the solvent.[17]

Analogously to Eisenberg et al.,[20] who constructed phase diagrams of PS-*b*-PAA aggregates in different solvents at room temperature, phase diagrams of PS_{139}-*b*-PAA_{17} in THF/H_2O mixtures at different temperatures were prepared based on the DLS data and the turbidity diagrams (**Figure 5**). The boundaries for different morphologies (or phases) are represented by connecting data points representing vesicles (empty circles), micelles (closed circles) or mixture of vesicles and micelles (circles with plus sign).

Figure 5a shows the transition from vesicles to micelles with different PS_{139}-*b*-PAA_{17} initial concentration at different temperatures. At high BCP concentrations the transition temperature shifts to higher values. The observation can be explained qualitatively by the change in the polymer-solvent interaction. As the polymer concentration goes up, the value of the interaction parameter χ increases.[17] Thus, at higher concentration the system needs to be heated to a higher temperature to cause a sufficient decrease in χ for the morphological change to take place. The same explanation can be applied on the system containing different THF contents, shown in Figure 5b. Here, however, one should notice that in pure water and at high water content no transition was observed in the temperature range in our experiments. This is tentatively attributed to the limited mobility of the hydrophobic PS under such conditions.

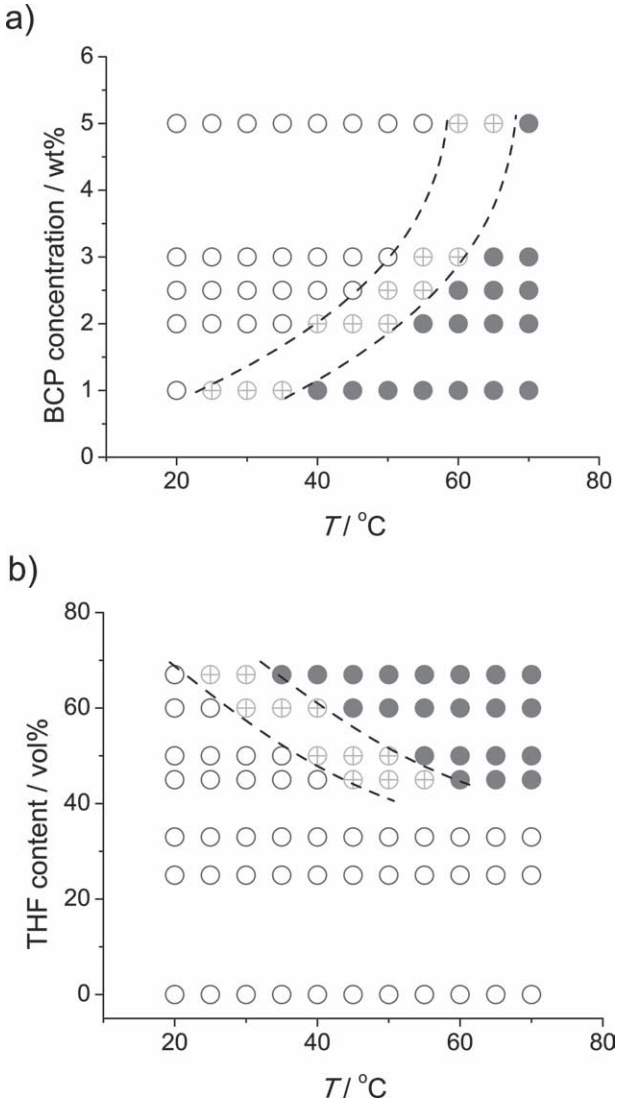

Figure 5. Phase diagrams of PS_{139}-*b*-PAA_{17} in THF/H_2O mixture at different temperatures. Empty circles stand for vesicles, filled circles for micelles, and circles with plus signs for mixture of vesicles and micelles.

2.3. Release and Encapsulation of Molecular Cargo Employing the Temperature-Induced Vesicle-To-Micelle Transition

The temperature-induced morphology changes described above can be exploited to i) release encapsulated molecules and ii) to partially re-encapsulate the reaction product. To demonstrate this unique features of the BCP system studied here, we utilized a two-step reaction, namely the hydrolysis of R110-Arg_2 catalyzed by trypsin,[21] and subsequently the quenching of the reaction product R110 by $NaNO_2$,[22] as also reported in a previous study (compare Scheme 1).[23] The kinetics of the enzymatic reaction as well as the quenching reaction is much slower than the transition kinetics (see Supporting Information), according to previous experiments.[23]

First PS-*b*-PAA vesicles (2 wt% BCP in THF, H_2O 50 vol%) with partly encapsulated R110-Arg_2 (total concentration 3.6 μM) were mixed with trypsin (c = 0.1 μM) at 20 °C. The sample was heated up to 50 °C after the absorption has reached steady state. After 5 h of heating the solution was cooled to 20 °C, followed by the addition of $NaNO_2$ (c = 1 mM). The absorbance of R110 at 495 nm was continuously monitored using UV–vis spectroscopy during the entire process (**Figure 6**, triangles). The exact same vesicle solution without the enzymes was used as a reference sample to correct for the effect of scattering. A control experiment with R110-Arg_2 and trypsin of the same concentration, but *without* any vesicles was also carried out (Figure 6, squares). The spectra shown in the insets display the absorption of R110 during the enzymatic reaction, as well as the quenching reaction.

In both curves the absorbance of R110 increased linearly in the first 4 hours before it gradually reached a plateau, indicating the complete conversion of all accessible (non-encapsulated) substrate molecules. In the case when part of the substrate molecules were encapsulated, the maximum absorbance was ~83% of the value of absorbance in the control sample. This difference is attributed to the encapsulation of R110-Arg_2 in the vesicles, which prevented the reaction with trypsin. The fraction of encapsulated substrate molecules (~17%) is in good agreement with previous results.[23] Heating to 50 °C (Figure 6a, grey bar) did not result in any significant changes of the absorbance of R110 in the control sample, while in the active sample the absorbance increased

small NANO MICRO

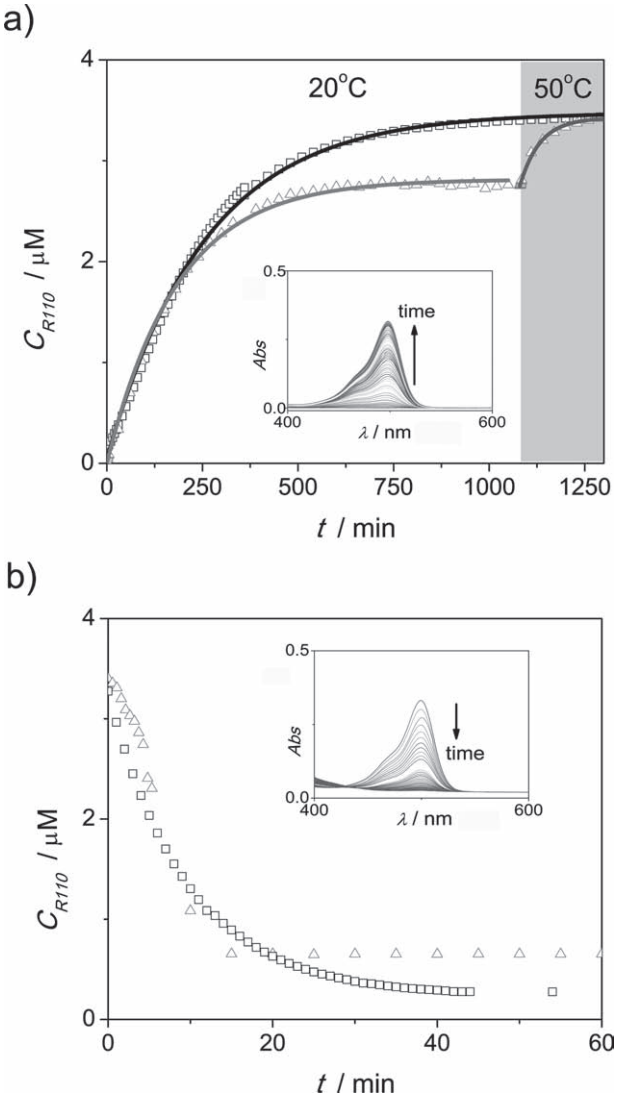

Figure 6. Plots of kinetics of a) the hydrolysis of R110-Arg_2 catalyzed by trypsin and b) the quenching reaction in the presence (triangles) and absence (squares) of PS-*b*-PAA vesicles (2 wt% BCP in THF, H_2O 50 vol%, D = 126 nm). The progress of the enzymatic reaction and the quenching reaction is also shown in the spectra shown in the insets.

to the same level as in the control sample. The observations indicate the conversion of the encapsulated R110-Arg_2 to R110, as a result from the vesicle-to-micelle transition, when the temperature was raised above the transition temperature. The addition of $NaNO_2$ after cooling the control sample to 20 °C resulted in a decrease of the absorbance to almost zero within 30 min. By contrast, in the active sample the absorbance remained at ~13% of its original value. This difference is attributed to the R110, which was encapsulated during the temperature-induced vesicle re-formation, as the vesicle wall was proven to impermeable to $NaNO_2$ in previous study[23] and thus prevented the quenching reaction.

The new strategy introduced in this report utilizes the temperature-induced vesicle-to-micelle transition of BCP aggregates to encapsulate and release small molecules. Temperature was thus used as an external stimulus to regulate the release of a reagent to allow (bio)chemical reactions to take place and the subsequent encapsulation of the product to protect it from unwanted interaction with other species.

We believe that this approach of assembly and disassembly of BCP vesicles across the transition temperature will provide a new pathway for temperature-controlled release of drugs or nutrients and should find potential applications in the fields such as therapeutics and medicine. The distinctive advantage of this system lies in the simplicity of synthesis and the possibility to fine-tune of the transition temperature by solution composition and/or a co-solvent. Compared to existing systems containing polymers with low critical solution temperature (LCST) behavior, this approach is truly complementary. Future research will focus on the exploration of alternative solvents and low glass transition temperature membrane forming polymers to widen the scope of applicability of these systems.

3. Conclusion

The size and morphology of PS-*b*-PAA aggregates in a THF/H_2O mixed solvent system was studied at different temperatures using TEM and light scattering. PS-*b*-PAA vesicles underwent a transition to micelles as the temperature was raised. The vesicle-to-micelle transition was attributed to the change in polymer solvent interaction at different temperatures, which was confirmed by varying the polymer concentration, as a higher polymer concentration would result in a larger value of the interaction parameter. Thus the system must be heated to a higher temperature to cause a sufficient decrease in interaction parameter for the vesicle-to-micelle transition. In addition, the presence of the common solvent THF was found to be crucial for the vesicle-to-micelle transition. Successful encapsulation and release of small molecules was achieved utilizing the assembly and disassembly of PS-*b*-PAA aggregates across the transition temperature. R110-Arg_2 was preloaded into the vesicles and released when the system was heated above the transition temperature to react with enzyme trypsin to form fluorescent product R110. The product was then encapsulated into reformed vesicles when the system was cooled down below the transition temperature, proven by the use of sodium nitrite.

4. Experimental Section

PS_{139}-*b*-PAA_{17} (the subscripts denote the number of repeat units for each block; number-averaged molecular weight, M_n = 15.7 kg/mol; polydispersity index = 1.07) was purchased from Polymer Source Inc. (Dorval, Canada). Bovine pancreas trypsin (TPCK Treated, essentially salt-free, lyophilized powder, ≥10 000 BAEE units/mg protein) and sodium nitrite were purchased from Sigma-Aldrich Co. (St. Louis, MO, USA). R110-Arg_2 were purchased from Molecular Probes/Invitrogen Co. (Carlsbad, CA, USA). All chemicals were used as received. THF (AR grade) was purchased from Biosolve B. V. (Valkenswaard, the Netherlands). Milli-Q water was produced by a Millipore Synergy system (Billerica, MA, USA).

PS-*b*-PAA vesicles were prepared by first dissolving the polymer in THF with various initial concentrations, then adding Milli-Q water as a precipitant into the polymer solution until a given water percentage was reached, while the entire system was under vigorous

stirring using a magnetic stirring bar with ~600 rpm at room temperature and subsequently heated to a designated temperature. Substrates were encapsulated in the vesicles by dissolving the substrates in water followed by immediate mixing. To follow the enzymatic reaction a further dilution was carried out to minimize the effect of scattering. To remove organic solvents dialysis was carried out using Spectra/Por 7 dialysis tubing from Spectrum Europe B.V. (Breda, the Netherlands) with a molecular weight cut off of 50 kD.

TEM images were acquired using an analytical TEM instrument Philips CM30 (FEI, Hillsboro, OR, USA) equipped with a post-column GIF Tridiem energy filter system (Gatan, Inc., Pleasanton, CA, USA). Samples for TEM were prepared by directly depositing a droplet of vesicle dispersion onto a carbon-coated TEM grid. After evaporation of the solvent the grid was fixed onto the specimen holder and mounted into the vacuum chamber.

The size of the PS-*b*-PAA aggregates was determined with a Malvern Zeta-sizer 4000 (Malvern Corp., Malvern, UK) at 25 °C using a laser wavelength of 633 nm and a scattering angle of 90°. The CONTIN method[24] was applied for data processing. The diameter, count rate and poly-dispersity index (PDI) of the aggregates were determined.

UV–vis spectra were recorded using a Varian Cary 300 Bio UV/Visible spectrophotometer (Varian, Inc. Palo Alto, CA, USA). A designated thermal mode was used to monitor the turbidity (absorbance at 400 nm) of the samples as a function of temperature. The enzymatic reaction was followed by monitoring the change in absorbance at 495 nm after the substrate-containing vesicles were mixed with enzymes. The same substrate-containing vesicle solution in the absence of enzyme was used as a reference sample to subtract the absorbance caused by scattering.

Supporting Information

Supporting Information is available from the Wiley Online Library or from the author.

Acknowledgements

This work was financially supported by the MESA+ Institute for Nanotechnology of the University of Twente (SRO Bionanotechnology).

[1] B. M. Discher, Y.-Y. Won, D. S. Ege, J. C.-M. Lee, F. S. Bates, D. E. Discher, D. A. Hammer, *Science* **1999**, *284*, 1143–1146.
[2] J. C. M. van Hest, D. A. P. Delnoye, M. W. P. L. Baars, M. H. P. Genderen, E. W. Meijer, *Science* **1995**, *268*, 1592–1595.
[3] L. F. Zhang, K. Yu, A. Eisenberg, *Science* **1996**, *272*, 1777–1779.
[4] J. J. L. M. Cornelissen, M. Fischer, N. A. J. M. Sommerdijk, R. J. M. Nolte, *Science* **1998**, *280*, 1427–1430.
[5] M.-H. Li, P. Keller, *Soft Matter* **2009**, *5*, 927–937.
[6] D. E. Discher, A. Eisenberg, *Science* **2002**, *297*, 967–973.
[7] F. H. Meng, Z. Y. Zhong, J. Feijen, *Biomacromolecules* **2009**, *10*, 197–209.
[8] Z. K. Zhou, B. Chu, D. G. Peiffer, *Macromolecules* **1993**, *26*, 1876–1883.
[9] Y. Fukumine, K. Inomata, A. Takano, T. Nose, *Polymer* **2000**, *41*, 5367–5374.
[10] S. V. Solomatin, T. K. Bronich, A. Eisenberg, V. A. Kabanov, A. V. Kabanov, *Langmuir* **2004**, *20*, 2066–2068.
[11] S. V. Aathimanikandan, E. N. Savariar, S. Thayumanavan, *J. Am. Chem. Soc.* **2005**, *127*, 14922–14929.
[12] Y. Li, B. S. Lokitz, C. L. McCormick, *Angew. Chem. Int. Ed.* **2006**, *45*, 5792–5795.
[13] Y. Li, A. E. Smith, B. S. Lokitz, C. L. McCormick, *Macromolecules* **2007**, *40*, 8524–8526.
[14] S. Qin, Y. Geng, D. E. Discher, S. Yang, *Adv. Mater.* **2006**, *18*, 2905–2909.
[15] K. E. Gebhardt, S. Ahn, G. Venkatachalam, D. A. Savin, *J. Colloid Interface Sci.* **2008**, *317*, 70–76.
[16] Y. F. Zhou, D. Y. Yan, W. Y. Dong, Y. Tian, *J. Phys. Chem. B* **2007**, *111*, 1262–1270.
[17] P. Bhargava, Y. Tu, J. X. Zheng, H. Xiong, R. P. Quirk, S. Z. D. Cheng, *J. Am. Chem. Soc.* **2007**, *129*, 1113–1121.
[18] I. LaRue, M. Adam, M. Pitsikalis, N. Hadjichristidis, M. Rubinstein, S. S. Sheiko, *Macromolecules* **2006**, *39*, 309–314.
[19] E. Feitosa, P. C. A. Barreleiro, G. Olofsson, *Chem. Phys. Lipids* **2000**, *105*, 201–213.
[20] H. Shen, A. Eisenberg, *J. Phys. Chem. B* **1999**, *103*, 9473–9487.
[21] S. P. Leytus, L. L. Melhado, W. F. Mangel, *Biochem. J.* **1983**, *209*, 299–307.
[22] X. Zhang, H. Wang, N. Fu, H. S. Zhang, *Spectrochim. Acta A* **2003**, *59*, 1667–1672.
[23] Q. Chen, H. Schönherr, G. J. Vancso, *Small* **2009**, *5*, 1436–1445.
[24] S. W. Provencher, *Biophys. J.* **1976**, *16*, 27–41.

Received: August 5, 2010
Published online: November 11, 2010

